Measuring water vapour permeability using remote-reading humidity sensors

Christopher Hall[1], **Gloria J Lo**[2], **Andrea Hamilton**[3]

[1]School of Engineering, University of Edinburgh, Edinburgh, UK

E-mail: christopher.hall@ed.ac.uk

[2]Department of Civil and Environmental Engineering, University of Strathclyde, Glasgow, UK

E-mail: glo.lo@strath.ac.uk

[3]Department of Civil and Environmental Engineering, University of Strathclyde, Glasgow, UK

E-mail: andrea.hamilton@strath.ac.uk

Abstract. The water vapour permeability is a material property used in calculations of the hygrothermal performance of buildings. The standard test method (the 'cup test'), little changed for decades and based on measuring weight changes, has been shown repeatedly in round-robin comparisons to have poor accuracy and little consistency between laboratories. Here we describe a new approach in which the primary measurement is of the humidity difference across the test sample, which is monitored continuously using sensors that are remotely readable. The box-in-box (BiB) apparatus described is smaller and simpler than that of the standard cup test. The BiB test is of shorter duration and is carried out without disturbance to the sample. New results on calcium silicate sheet, brick ceramic and autoclaved aerated concrete are compared with published vapour permeability values obtained by the standard test (considered to be of lower accuracy).
[*142 words*]

Keywords: water vapour permeability, water vapour diffusivity, cup test, humidity, humidity sensor, porous materials

Submitted to: *Meas. Sci. Technol.* as a **Technical Note**

1. Introduction

The water vapour permeability D_v is the property of a porous material that defines the rate of transport of water vapour in a gradient of vapour pressure p_w (or relative humidity RH) at a fixed temperature T. This property is used widely in building physics [1, 2], particularly in models of the hygrothermal behaviour of building structures. Values of D_v are required in

associated design methods, for example for the moisture buffering of internal spaces [3]. This is the context of the work reported here. Water vapour transmission is also important in textile, paper and packaging technologies, in biological, environmental and biomedical transpiration physics [4, 5].

In the widely used method of measuring D_v, little changed from that described by Joy and Wilson in 1963 [6], a cup containing a saturated salt solution is capped with a specimen of the test material and placed in an environmental chamber. Inside the cup the saturated salt solution establishes a fixed RH, which by the phase rule remains constant so long as both solid salt and saturated solution are present together, irrespective of the amount of water. Thus the solution acts as a humidistat and a source or sink of water at constant vapour pressure p_w. The environmental chamber is maintained at a different constant RH, either by using a different saturated salt solution or more commonly by using a dynamically controlled water injection system. By this arrangement a gradient of water vapour pressure is established across the test specimen, and water vapour then diffuses through the test specimen from the higher RH to the lower RH. The rate of transfer is determined by weighing the cup from time to time, and from such data the vapour permeability is estimated. This arrangement, generally known as the 'cup test', is described in several standards [7, 8].

Despite its long history of use, the cup test has been shown repeatedly in round-robin studies to be of poor reproducibility [9, 10, 11, 12]. While numerous sources of error have been identified, notably in [6, 13, 14, 15], the most intractable is that of controlling (or of knowing) the RH at each face of the specimen. Without constant and precisely known boundary conditions on the specimen surfaces, the test procedure fails to match the underlying theory of its operation. This difficulty is inherent in the experimental arrangement: since there is a finite water flux through the specimen, there must necessarily be gradients of water vapour pressure (or RH) not only across the specimen but also between the specimen and the surface of the salt solution in the cup, and across the boundary layer adjacent to the specimen in the environmental chamber. But in the standard cup test, the water vapour pressures at or near the surfaces of the test specimen are not measured, and the accuracy of the estimate of D_v is immediately compromised. The poor reproducibility then arises because the true boundary condition at the specimen surface depends in an uncontrolled manner on the internal circulation of water vapour in both cup and environmental chamber, neither of which is adequately specified in standard tests.

In the new test described here, we circumvent this difficulty by making continuous RH measurements close to the two surfaces of the specimen.

2. Theory

In the simple schematic of figure 1, we show a mass flux of water j_m through a porous barrier separating two compartments A and B in which the water vapour pressure is maintained at different constant values $p_{w\mathrm{A}}$, $p_{w\mathrm{B}}$. The total pressure P_0 is the same on both sides of the

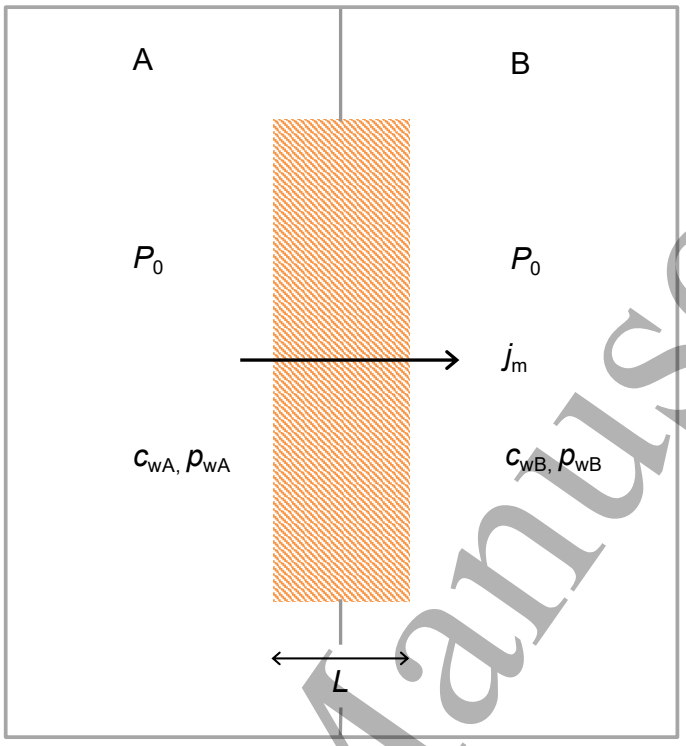

Figure 1. Diffusive mass flux j_m of water vapour through a permeable barrier of thickness L separating two compartments A and B with water vapour concentrations $c_{w\mathrm{A}} > c_{w\mathrm{B}}$, vapour pressures $p_{w\mathrm{A}} > p_{w\mathrm{B}}$, and total gas pressure P_0.

barrier, and the system is isothermal with temperature T. By Fick's law, we have

$$j_m = -D_w \frac{dc_w}{dx}, \tag{1}$$

where c_w is the gas phase water concentration and D_w is a diffusivity with dimension $\mathsf{L}^2\mathsf{T}^{-1}$. Provided that water transport in the barrier occurs solely by molecular diffusion in the gas phase we can regard D_w as the water vapour diffusivity of the barrier. Now we note that the mass concentration c_w is equal to the vapour density of water ρ_v. Assuming ideal behaviour we have $\rho_v = p_w M/(\mathbf{R}T)$ where M is the molar mass of water, and T the absolute (kelvin) temperature, so that

$$j_m = -\frac{D_w M}{\mathbf{R}T}\frac{dp_w}{dx} = -D_v \frac{dp_w}{dx} = D_v \frac{p_{w\mathrm{A}} - p_{w\mathrm{B}}}{L}, \tag{2}$$

where the lumped quantity $D_v = D_w M/(\mathbf{R}T)$ is called the water vapour permeability, with dimension T. In building physics, D_v is often denoted δ_p, but here we follow the notation of [16]. The vapour transport resistance factor $\mu = D_{w0}/D_w$, where D_{w0} is the water vapour diffusivity in still air at the same temperature T and pressure P_0.

Remark. As noted elsewhere [16], the flux is purely diffusive and there is no advection in the barrier. Therefore D_v is not a permeability in the Darcian sense, but is a quantity proportional to the binary molecular diffusivity D_w. However the terminology is long established and we

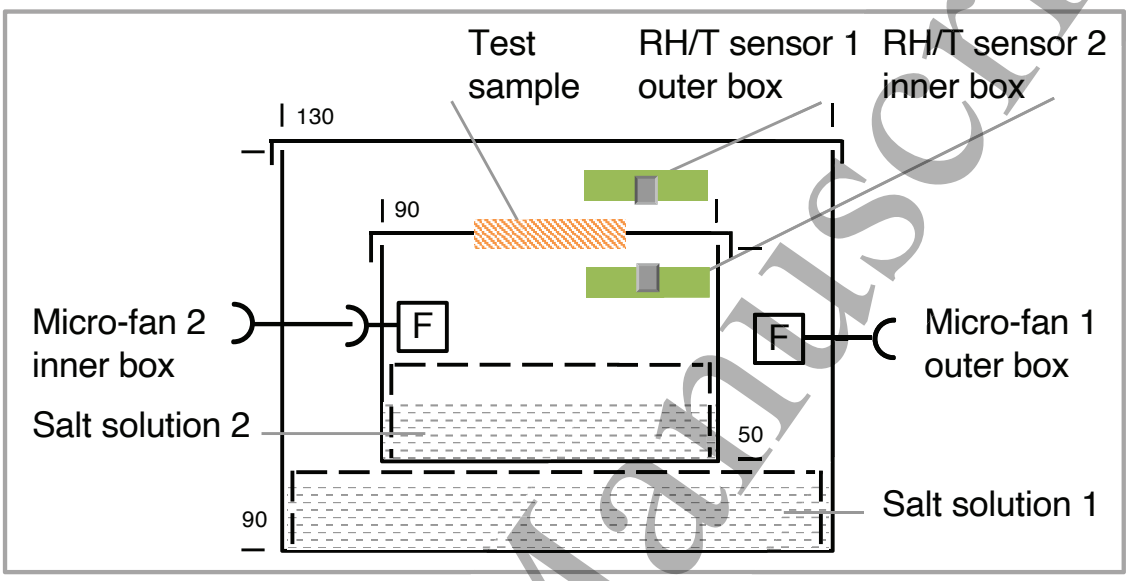

Figure 2. Test apparatus: Box-in-box saturated salt solution humidistats, each box with a remote-reading humidity/temperature sensor (Sensirion SHT4x) and a micro-fan (1 Sunon UF3C3, 2 UB393); box dimensions $l \times w \times d$ (mm), Inner Box $110 \times 90 \times 50$, Outer Box $180 \times 130 \times 90$, ($w \times d$ shown).

follow it here. In the case of water vapour in air at normal environmental temperatures and pressures, the partial pressure of water vapour p_w rarely exceeds 0.04 atm and is often much less. Water is therefore a dilute component of the gas phase and D_w may be regarded as the tracer diffusivity of water vapour in air within the barrier material.

3. Concept and design

In the standard test [17, 7, 8], the primary data are the weights of the cup measured from time to time to monitor the progressive transfer of water through the sample. As we have noted, among several practical difficulties, the most intractable is the absence of any satisfactory control of the humidity gradient across the sample.

In the box-in-box (BiB) device we describe here and shown in figure 2, the inner box is also a humidistat, with the test material set into the lid of the box. The outer box is a second humidistat providing a different RH. To that extent only the BiB test resembles the standard cup test, with the environmental chamber replaced by a second saturated salt solution humidistat. In all other respects the BiB test and the cup test are markedly different. In the BiB test, the primary data are not weights but are the humidities in the two boxes, measured

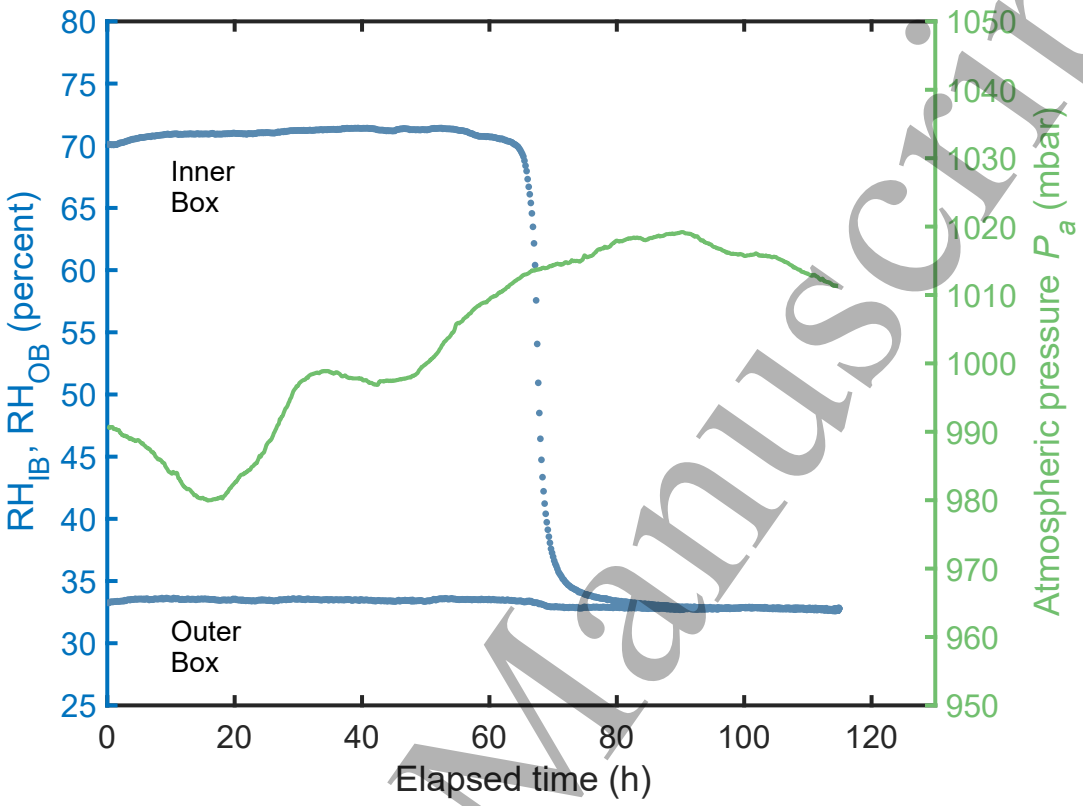

Figure 3. Raw data from a BiB test: AAC sample, 25 °C, using $MgCl_2.6H_2O$ (OB) (RH 32.8±0.2 percent), and NaCl (IB) (RH 75.3±0.1 percent) saturated salt solution humidistats. Atmospheric pressure variation is also shown.

continuously with remote-reading sensors. The sensors measure both RH and temperature at preset intervals, say every 5 min. Each RH sensor is located close to the sample surface, so that the difference in RH across the sample $\Delta(\mathrm{RH})_{\mathrm{IB/OB}}$ is measured directly throughout the course of the test. In addition, each box is fitted with a micro-fan to circulate air across the sample surface. The boxes are placed in a temperature-controlled enclosure for the duration of the test. The primary data are the RH measurements at each side of the test sample, as shown in figure 3. At the start of a test a precisely measured mass of water (typically 0.5–1 g) is added to the large excess of solid salt in the InnerBox before it is closed. The test runs until all the water is completely transferred from the Inner Box to the Outer Box, as indicated by the RH sensors. We note that at a given temperature T the solid salt + saturated solution + vapour is thermodynamically invariant, and has constant water vapour pressure at the solution surface so long as there is any water present.

The use of remote-reading RH sensors brings great advantages, which we have exploited previously in a device for measuring rates of evaporation [18]. A remote-reading sensor has been recently used to measure the RH inside the cup of a standard vapour permeability test [19, 20], showing the existence of an RH gradient inside the cup. This contributes to the

poor control of the RH at the sample surface, the troublesome defect of the the standard cup test.

The BiB test of figure 2 is compact, with the OuterBox only 190 × 130 × 90 mm, much smaller than standard cup test apparatus. The reduction in size, and the use of micro-fans, tends to increase the diffusive flux through the specimen and to shorten the duration of the test. The test runs described here were complete in 40–80 h.

3.1. Materials

Three materials have been used: a calcium silicate board denoted HCS, an autoclaved aerated concrete AAC; and a fired-clay ceramic brick HBC. All three are commercial materials, and to allow comparison with prior published data they are the same materials that were used in the Hamstad round-robin study of 2001–2003 [11]. The HCS and HBC materials used are from the same stock of materials that was distributed for the Hamstad project. In the case of AAC, measurements were made on newly acquired material from the same manufacturer, and having similar density and porosity as the original Hamstad material. The three materials have diverse compositions and physical properties. HCS, widely used as a thermal insulant, consists mainly of fibres of the hydrothermal mineral xonotlite, with small amounts of calcite and cellulose [21, 22]. Its open fibrous microstructure has an unusually low packing density and high volume-fraction porosity [16]. In AAC, a structural masonry material, the binding component is the hydrothermal mineral tobermorite-11Å [23], which is combined with sand and small quantities of other minerals [24]. The material has a bimodal pore structure in which large bubbles are dispersed in a fine-grained matrix [25]. Although the porosity is high the coarse pores are only weakly interconnected, mainly through the fine pores. The HBC brick ceramic is typical of machine-made clay bricks: the complex mineralogy reflects noncalcareous raw materials [26], and the porosity and bulk density are roughly mid-range for modern commercial bricks [27]. HBC is non-hygroscopic, and HCS and AAC are only weakly hygroscopic, with less than 1.5 percent mass fraction water content at 50 percent RH (25 °C). The contribution to the total flux from capillary transport is considered negligible. Data on physical properties are collected in Table 1.

3.2. Test procedures

In the tests reported here the Inner Box humidistat (figure 2) was established with a saturated solution of sodium chloride NaCl (RH 75.3±0.1 percent) made by adding water to a large excess of solid salt. In the Outer Box magnesium chloride hexahydrate $MgCl_2.6H_2O$ (RH 32.8±0.2 percent) was used. Reference data on the equilibrium RH values of these and other saturated salt humidistats are provided by Greenspan [28]. Values from other sources of data [29, 30] are similar. The relative humidities in the Inner and Outer boxes give an RH difference across the sample of about 40 percent with a mean RH of about 50 percent. These values are typical of conditions within construction elements and adjacent spaces. Other humidistats can be selected to suit the needs of the user [31]. All tests were run at 25±0.2 °C. Test samples were conditioned at the Outer Box RH in order that the sorbed water content

Table 1. Physical properties of materials

Material	Bulk density ρ_b	Solid density ρ_s	Porosity f	Mass fraction water content at 50 percent RH $\theta_{m,50}$
	kg/m^3	kg/m^3	[-]	[-]
HCS	270	2540	0.895	0.0093
AAC	475	2530	0.813	0.0125
HBC	2005	2630	0.238	0.00023

Notes: (1) Values of ρ_b, ρ_s, f from [11]; values of $\theta_{m,50}$ (25 °C) are calculated from authors' sorption isotherm data (unpublished). Standard uncertainties: ρ_b, ρ_s 5 kg/m^3; f 0.002; $\theta_{m,50}$ HCS, AAC 0.002, HBC 0.00007.

should be the same at the beginning and the end of a test run. In any case, as shown in Table 1 the mass-fraction water content of all the materials used is extremely small. The RH/T sensors were calibrated individually. They were found to be stable; calibration corrections were in the range ±0.7 percent RH. Sensors were conditioned before tests in the appropriate humidistat. The micro-fans delivered a circulatory airflow of 1.2 L/min (IB) and 6.0 L/min (OB) at maximum speed but were operated at about one-quarter speed by means of DC buck converters on the 3V input voltage. The Inner Box had a volume of about 180 mL, the Outer Box 470 mL.

3.3. Data analysis

From the primary RH data shown in figure 3, we calculate the RH difference $\Delta(\mathrm{RH})_{\mathrm{IB/OB}}$ across the sample, as shown in figure 4. This is roughly constant for most of the test, and then reduces rapidly as the quantity of water in the Inner Box approaches zero. This roll-off is not caused by a change in the water vapour pressure at the surface of the solution but rather by a reduction in the area of solution surface supplying water vapour. However, we continue to measure $\Delta(\mathrm{RH})_{\mathrm{IB/OB}}$ throughout the test, and then make a numerical estimate of the integral

$$I = \int_{t_1}^{t_2} \Delta(\mathrm{RH})_{\mathrm{IB/OB}} dt, \tag{3}$$

where t_1, t_2 are the start and end times of the test run. The water vapour permeability D_v is then:

$$D_v = \frac{100 m_w L}{A I p_{w0}}, \tag{4}$$

where p_{w0} is the saturated vapour pressure of water at temperature T, m_w is the mass of water used, L is the sample thickness and A the sample area.

It is good practice to report the permeability at the standard atmospheric pressure at sea level of 1 atm, $P_{a0} = 101325$ Pa. We record also the atmospheric pressure P_a throughout the

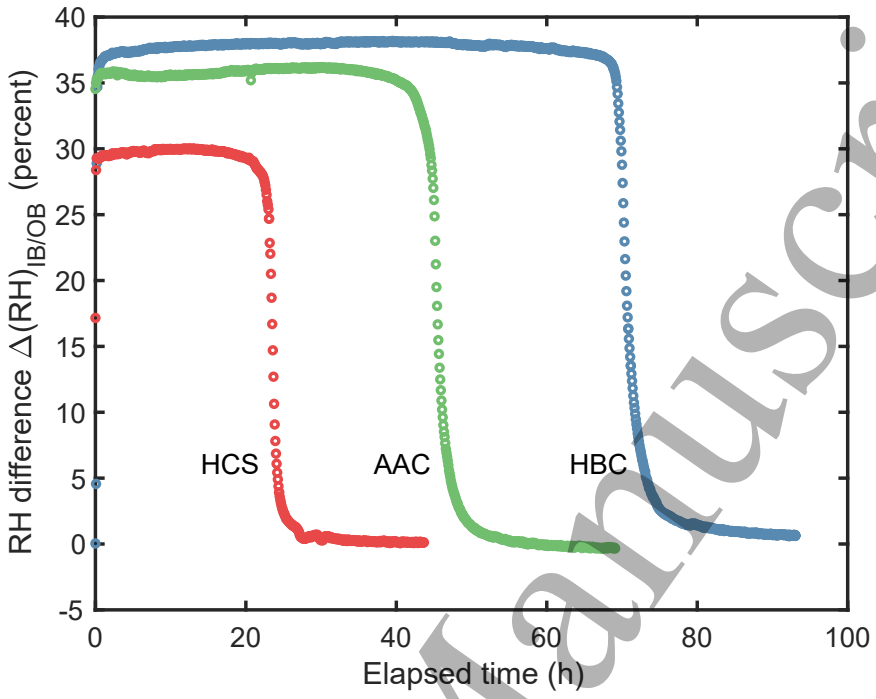

Figure 4. Measured variation of $\Delta(\mathrm{RH})_{\mathrm{IB/OB}}$ for materials HAC, AAC and HCB during test runs at 25 °C.

test, most conveniently using a Tempo sensor disc which like the RH/T sensors is remotely readable. If the mean atmospheric pressure measured in the test run is $\bar{P}_a$, then the adjusted value of the permeability is $D_{v,atm} = D_v \bar{P}_a / P_{a0}$. The value of $\bar{P}_a$ is weighted by $\Delta(\mathrm{RH})_{\mathrm{IB/OB}}$. The diffusivity $D_w = D_v(\mathbf{R}T)/M$ is likewise adjusted to standard atmospheric pressure, $D_{w,atm} = D_w \bar{P}_a / P_{a0}$. The resistance factor μ is independent of pressure (and also of temperature).

We note that the variation of atmospheric pressure over the duration of a test run is usually small, typically less than 2 percent. However, larger deviations from the standard atmosphere may occur for reasons of geographical elevation.

A small correction to the initial mass of water is sometimes made to allow for leakage from the box. In our tests this was very small, about 2×10^{-5} g/(h percent RH), and can be reduced to a value close to zero by using an additional silicone rubber gasket (cut from 0.2 mm thick sheet, Silex Ltd UK) between the seals of the lid.

3.4. Performance

Results of a series of tests are compiled in Table 2. The values of D_w and D_v are derived from datasets such as are shown in figure 4. A notable feature of the data is the clear dependence of $\Delta(\mathrm{RH})_{\mathrm{IB/OB}}$ on the resistance factor μ of the material. The IB RH of HBC is some 7 percent higher than that of HCS, indicating a marked difference in the RH gradient between the sample

Table 2. Water vapour transport properties measured at 25.0±0.2 °C.

Material	water vapour diffusivity $D_{w,atm}$ 10^{-6}m^2/s	water vapour permeability $D_{v,atm}$ 10^{-11}s	Resistance factor μ [-]
HCS	9.51±0.11	6.91±0.08	2.68±0.03
AAC	2.00±0.04	1.45±0.02	12.7±0.2
HBC	1.40±0.02	1.02±0.02	18.2±0.3

Notes: Means of three replicate tests on each material; $D_{w,atm}$, $D_{v,atm}$ are values at 1 atm standard pressure. In calculating D_w, the value of $p_{w0} = 3170$ kPa at 25 °C is used [16]; in calculating μ, the value of $D_{w0} = 25.5 \times 10^{-6}$ m^2/s at 1 atm pressure and 25 °C is used [32, 16]; $M/(\mathbf{R}T) = 7.2672\times10^{-6}$ s^2/m^2 at 25 °C.

and the surface of the saturated salt solution. In the standard test it is necessary to estimate that gradient (and the associated mass transfer resistance) by means of supplementary tests [7]. In the BiB test, this is no longer required since the RH at each sample surface is measured directly.

In figure 5 the measured values of resistance factor μ for HCS, AAC and HBC are shown, together with published values. The values from the Hamstad round-robin [11] show great scatter. Indications are that the BiB test delivers values that are consistent with earlier measurements, and that replicate values have much smaller scatter.

4. Conclusions

The new test for determining the water vapour permeability that we describe has five advantages over the standard cup test. These are that

- the raw RH data are logged continuously, providing much greater data density than manual weighings;
- acquiring RH data at or close to the sample surface largely circumvents the problems of estimating resistances within the chamber and cup;
- the incorporation of micro-fans in both boxes reduces gradients of RH;
- the duration of the test is reduced from several weeks to several days;
- the test runs unattended, and there is no disturbance to the sample during the test.

Acknowledgments We thank Jianhua Zhao for unpublished data on HBC, HCS resistance factors.

References

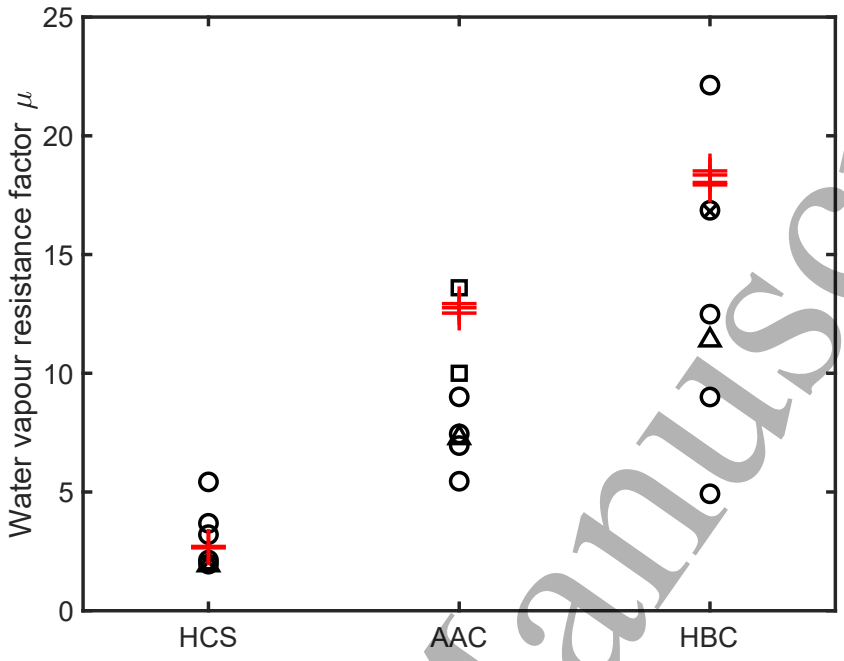

Figure 5. Comparison of BiB values of resistance factor μ (+) with published values: △ [33]; □ [34]; ○ [11], × [35]. The plotted values of published data are interpolations to the mean RH of the BiB tests, 54.2 percent. Additional unpublished data from J Zhao were used to calculate interpolated values for HCS, HBC from [35] .

[1] Hens H. S. L. C. (2006). The vapor diffusion resistance and air permeance of masonry and roofing systems. *Building and Environment*, **41**, 745–755.

[2] Hens H. S. L. C. (2015). Combined heat, air, moisture modelling: a look back, how, of help? *Building and Environment*, **91**, 138–151.

[3] Hall C., Lo G. J. and Hamilton A. (2021). Sharp Front analysis of moisture buffering. *RILEM Technical Letters*, **6**, 78–81.

[4] Stroock A. D., Pagay V. V., Zwieniecki M. A. and Holbrook N. M. (2014). The physicochemical hydrodynamics of vascular plants. *Annual Review of Fluid Mechanics*, **46**, 615–642.

[5] Duan Z., Jiang Y. and Tai H. (2021). Recent advances in humidity sensor for human body related humidity detections. *Journal of Materials Chemistry C*, **9**, 14963–14980

[6] Joy F. A. and Wilson A. G. (1963) Standardization of the dish method for measuring water vapor transmission. *Proceedings of the International Symposium on Humidity and Moisture*, Washington DC 1963, **4**, pp 259—270. (Division of Building Research paper no 279, National Research Council Canada 1966).

[7] ISO 12572:2016. *Hygrothermal performance of building materials and products – Determination of water vapour transmission properties – Cup method*.

[8] ASTM E96-16. *Standard test methods for water vapor transmission of materials*.

[9] Galbraith G. H., McLean R. C. and Tao Z. (1993). Vapour permeability: suitability and consistency of current test procedures. *Building Services Engineering Research and Technology*, **14**, 67–70.

[10] Kumaran M. K. (1998). Interlaboratory comparison of the ASTM standard test methods for water vapor transmission of materials (E 96-95). *Journal of Testing and Evaluation*, **26**, 83–88.

[11] Roels S., Carmeliet J., Hens H., Adan O., Brocken H., Cerny R., Pavlik Z., Hall C., Kumaran K., Pel L. and Plagge R. (2004) Interlaboratory comparison of hygric properties of porous building materials. *Journal*

of Thermal Envelope and Building Science, **27**, 307–325.

[12] Feng C., Guimarães A. S., Ramos N., Sun L., Gawin D., Konca, P., Hall C., Zhao J., Hirsch H., Grunewald J., Fredriksson M., Hansen K. K., Pavlík Z., Hamilton A. and Janssen H. (2020). Hygric properties of porous building materials (VI): A round robin campaign. *Building and Environment*, **185**, 107242.

[13] Bomberg M. (1989) Testing water vapor transmission: Unresolved issues. In *Water vapor transmission through building materials and systems: Mechanisms and measurement*, STP 1039, ASTM, pp. 157–167.

[14] Galbraith G. H., McLean R. C., Tao Z. and Kang N. (1992) The comparability of water vapour permeability measurements.*Building Research and Information*, **20**, 364–372.

[15] Hens H. S. L. C. (2009). Vapor permeability measurements: impact of cup sealing, edge correction, flow direction, and mean relative humidity. *Journal of ASTM International*, **6**, 101893.

[16] Hall C. and Hoff W. D. (2021) *Water transport in brick, stone and concrete*, 3rd edn, CRC Press, London and New York.

[17] Fanney A. H., Thomas W. C., Burch D. M. and Mathena L. R. Jr. (1991) Measurements of moisture diffusion in building materials. *ASHRAE Transactions*, **97**, 99–113.

[18] Hall C. and Hamilton A. (2020). A device for the local measurement of water evaporation rate. *Measurement Science and Technology*, 31, 127001.

[19] Colinart T. and Glouannec P. (2021). Water vapor permeability of building materials: improved analysis of dry cup experiment. *1st International Conference on Moisture in Buildings (ICMB21)*, UCL London 28-29 June 2021.

[20] Colinart T. and Glouannec P. (2022). Accuracy of water vapor permeability of building materials reassessed by measuring cup's inner relative humidity. *Building and Environment*, **217**, 109038.

[21] Hamilton A. and Hall C. (2005) Physicochemical characterization of a hydrated calcium silicate board material. *Journal of Building Physics*, **29**, 9–19.

[22] Hamilton A. and Hall C. (2007) A note on the density of a calcium silicate hydrate board material. *Journal of Building Physics*, **31**, 69–71.

[23] Mitsuda T., Sasaki K. and Ishida, H. (1992). Phase evolution during autoclaving process of aerated concrete. *Journal of the American Ceramic Society*, **75**, 1858–1863.

[24] Paul M. (2018). Quality control of autoclaved aerated concrete by means of X-ray diffraction. *ce papers*, **2**, 111–116.

[25] Ioannou I., Hamilton A. and Hall C. (2008) Capillary absorption of water and *n*-decane by autoclaved aerated concrete. *Cement and Concrete Research*, **38**, 766–771.

[26] Dunham A. C., McKnight A. S. and Warren I. (2001) Mineral assemblages formed in Oxford Clay fired under different time–temperature conditions with reference to brick manufacture. *Proceedings of the Yorkshire Geological Society*, **53**, 221–230.

[27] Hall C. and Hamilton A. (2015) Porosity–density relations in stone and brick materials. *Materials and Structures*, **48**, 1265–1271.

[28] Greenspan L. (1977) Humidity fixed points of binary saturated aqueous solutions. *Journal of Research of the National Bureau of Standards*, **81A**, 89–96.

[29] Pollio M. L., Kitic D., and Resnik S. L. (1996) Research note: A_w values of six saturated salt solutions at 25 °C. Re-examination for the purpose of maintaining a constant relative humidity in water sorption measurements. *LWT-Food Science and Technology*, **29**, 376–378.

[30] ASTM E104-02. *Standard practice for maintaining constant relative humidity by means of aqueous solutions*.

[31] Olaoye T. S., Dewsbury M. and Künzel, H. (2021). Laboratory measurement and boundary conditions for the water vapour resistivity properties of typical Australian impermeable and smart pliable membranes. *Buildings*, **11**, 509.

[32] Massman W. J. (1998) A review of the molecular diffusivities of H_2O, CO_2, CH_4, CO, O_3, SO_2, NH_3, N_2O, NO and NO_2 in air, O_2 and N_2 near STP. *Atmospheric Environment*, **32**, 1111–1127.

[33] Feng C. and Janssen H. (2021). Hygric properties of porous building materials (VII): Full-range benchmark characterizations of three materials. *Building and Environment*, **195**, 107727.

[34] Jerman M., Keppert M., Výborný J. and Černý R. (2013). Hygric, thermal and durability properties of autoclaved aerated concrete. *Construction and Building Materials*, **41**, 352–359.

[35] Zhao J., Feng S., Grunewald J., Meissner F. and Wang J. (2022). Drying characteristics of two capillary porous building materials: Calcium silicate and ceramic brick. *Building and Environment*, **216**, 109006.